ORGANIC LETTERS

2011
Vol. 13, No. 16
4450–4453

New Chiral Cyclooctatriene-Based Polycyclic Architectures

Grégory Pieters,[†] Anne Gaucher,*[,†] Jérôme Marrot,[†] François Maurel,[‡] Jean-Valère Naubron,[§] Marion Jean,[§] Nicolas Vanthuyne,[§] Jeanne Crassous,[∥] and Damien Prim*[,†]

Université de Versailles-Saint-Quentin-en-Yvelines, Institut Lavoisier de Versailles, UMR CNRS 8180, 45 Avenue des Etats-Unis, F-78035 Versailles, France, Sciences Chimiques de Rennes, UMR CNRS 6226, Université de Rennes 1, Campus de Beaulieu, Av. du Général Leclerc, F-32045 Rennes Cedex, France, Université Paul Cézanne – Spectropole & UMR CNRS 6263 – Case A62 Avenue Escadrille Normandie-Niémen 13397 Marseille Cedex 20, France, and Laboratoire Interfaces, Traitements, Organisation et Dynamique des Systèmes (ITODYS), CNRS UMR 7086, Université Paris 7 - Paris Diderot, Bâtiment Lavoisier, 15 rue Jean Antoine de Baïf, 75205 Paris Cedex 13, France

prim@chimie.uvsq.fr; anne.gaucher@chimie.uvsq.fr

Received July 6, 2011

ABSTRACT

The synthesis and properties of new chiral polycyclic architectures that display both helicity and a saddle-type shape are described. The enantiomers have been separated, and their absolute configuration was determined by VCD and ECD. The unprecedented molecular architecture is based on a cyclooctatriene core surrounded by an association of benzo[*c*]fluorene and *ortho*-phenylene units.

Unusual topologies of polycyclic hydrocarbons have been the subject of continuous and considerable attention. Within this large family of chemical compounds, architectures based on a central ring surrounded by several cyclic subunits are of particular interest mainly because such molecules display various shapes such as planar (PL), bowl-shaped (BS), or saddle-shaped (SS).[1] If the central ring size deeply impacts the overall shape, it may be affected or even modified by several additional parameters such as (i) the surrounding lattice of fused aromatics, (ii) the substitution of a six- by a five-membered ring in the outer circular arrangement, and (iii) rupture of annelation and introduction of sp^3-hybridized carbon atoms. For example, in the circulene series, moving from [5]- to [6]- and further [7]-circulene induces shape modifications from BS to PL and further to SS respectively.[2] PL [6]-circulene and BS sumanene differ from each other by the ring size of some surrounding cycles.[3] In this context, five-, six-, or seven-membered central rings are common cores. In contrast, the next higher eight-membered homologues are so far less described. The most prominent examples described in the literature appear to be highly symmetrical molecules

[†] Université de Versailles-Saint-Quentin-en-Yvelines.
[‡] Université Paris 7 - Paris Diderot.
[§] Université Paul Cézanne.
[∥] Université de Rennes 1.

(1) For a recent review, see: Hoheisel, T. N.; Schrettl, S.; Szilluweit, R.; Frauenrath, H. *Angew. Chem., Int. Ed.* **2010**, *49*, 6496.

(2) (a) Steinberg, B. D.; Jackson, E. A.; Filatov, A. S.; Wakamiya, A.; Petrukhina, M. A.; Scott, L. T. *J. Am. Chem. Soc.* **2009**, *131*, 10537. (b) Boedigheimer, H.; Ferrence, G. M.; Lash, T. D. *J. Org. Chem.* **2010**, *75*, 2518. (c) Yamamoto, K.; Harada, T.; Nakazaki, M.; Nakao, T.; Kai, Y.; Harada, S.; Kasai, N. *J. Am. Chem. Soc.* **1983**, *105*, 7171.

(3) (a) Sakurai, H.; Daiko, T.; Sakane, H.; Amaya, T.; Hirao, T. *J. Am. Chem. Soc.* **2005**, *127*, 11580. (b) Yamamoto, K.; Harada, T.; Okamoto, Y.; Chikamatsu, H.; Nakazaki, M.; Kai, Y.; Nakao, T.; Tanaka, M.; Harada, S.; Kasai, N. *J. Am. Chem. Soc.* **1988**, *110*, 3578.

10.1021/ol201804h
Published on Web 07/26/2011

such as the nonplanar tetraphenylene,[4] several bridged tetraphenylenes,[5] and the planar octathio[8]circulene, also called sulflower.[6]

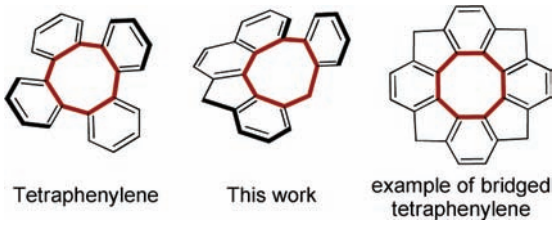

Figure 1. Polycyclic architectures based on an eight-membered ring.

We report herein the synthesis of new polycyclic hydrocarbon architectures containing a central eight-membered ring that bridges four six-membered and one five-membered unit together as illustrated in Figure 1. In addition to the short synthesis, the structural determination, the computed reaction pathway, and conformational barriers are described. For **6**, the enantiomers were separated by chiral HPLC, their absolute configurations were assigned using VCD, ECD, their chiroptical properties, and enantiomerization barriers were determined.

Scheme 1. Synthesis of Polycyclic Architectures

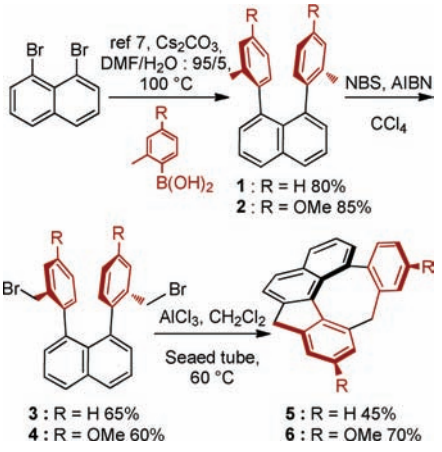

Our approach relies upon a key double electrophilic aromatic cyclization to install both the five- and eight-membered rings. Precursors **3** and **4** are easily obtained in two steps starting from 1,8-dibromonaphthalene as recently described (Scheme 1).[7] Benzylic carbocations are generated upon treatment with Lewis acids and undergo electrophilic aromatic substitutions featuring the construction of target architectures.

Refluxing **3** in DCM, in the presence of a catalytic amount of aluminum chloride, afforded a complete conversion after 24 h. ^{1}H NMR spectra confirmed the presence of a nonsymmetrical structure containing both a cyclopentadiene and a cyclooctatriene unit (see Supporting Information (SI)). Under Friedel–Crafts alkylation conditions, **3** afforded compound **5** in a fair 45% yield. Gratifyingly, the constrained helical architecture **6** was selectively obtained in a high 70% yield, starting from bismonobromodiarylnaphthalene **4**. Crystals suitable for single crystal X-ray diffraction analysis could be obtained from slow evaporation of a chloroform solution of **5** (Figure 2).

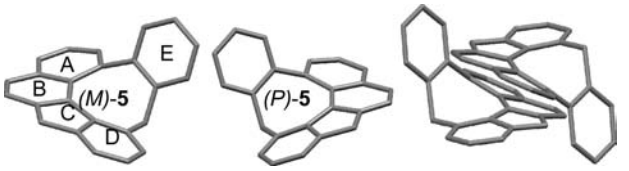

Figure 2. Single crystal X-ray diffraction analysis of constrained architecture **5**.

The joint presence of the benzo[*c*]fluorene unit, the cyclooctatriene core, and the benzylic moiety imposes the twisting of the A, B, C, D ring sequence, which accounts for the helical fragment of the architecture. Examination of **5** in the solid state deserves some additional comments: (i) The presence of both *P* and *M* enantiomers, as shown in Figure 2, confirmed the chiral nature of the architecture. (ii) Edge-to-face interactions between the orthogonal E and C rings as well as weak $\pi-\pi$ interactions between two orthogonal E rings of each molecule set the design of the dimeric arrangement. Within this set, both perpendicular E rings and cyclooctatriene units arranged *anti* to each other with regards to the central A, B, C, D ring sequence (Figure 2).

The nonplanar conformation of the cyclooctatriene moiety forces the E ring to adopt an almost perpendicular position with regards to the condensed A, B, C, D. The association of both cyclooctatriene and the perpendicular isolated *ortho*-phenylene ring is responsible for the curvature region in **5**. Thus, both substructures impact the flexibility, torsion, and overall design of the molecular architecture. During the $AlCl_3$ promoted double electrophilic aromatic cyclization, both the five- and the eight-membered rings are generated. The molecular architecture of **5** and **6** is due to the selective formation of the five-/eight-membered ring combination over a plausible five-/five-membered ring system.

This unusual combination posed the question of the reaction pathway and more precisely which ring (five or

(4) For recent literature, see: (a) Rajca, A; Rajca, S. *Angew. Chem., Int. Ed.* **2010**, *49*, 672. (b) Hilton, C. L.; Crowfoot, J. M.; Rempala, P.; King, B. T. *J. Am. Chem. Soc.* **2008**, *130*, 13392. (c) Iglesias, B.; Cobas, A.; Pérez, D.; Guitian, E. *Org. Lett.* **2004**, *6*, 3557.

(5) (a) Hellwinkel, D.; Reiff, G. *Angew. Chem.* **1970**, *82*, 516. (b) Hellwinkel, D.; Reiff, G.; Nykodym, V. *J. Liebigs Ann. Chem.* **1977**, 1013.

(6) Chernichenko, K. Y.; Sumerin, V. V.; Shpanchenko, R. V.; Balenkova, E. S.; Nenajdenko, V. G. *Angew. Chem., Int. Ed.* **2006**, *45*, 7367.

(7) (a) Pieters, G.; Gaucher, A.; Prim, D.; Marrot, J. *Chem. Commun.* **2009**, 4827. (b) Pieters, G.; Terrasson, V.; Gaucher, A.; Prim, D.; Marrot, J. *Eur. J. Org. Chem.* **2010**, *30*, 5800.

eight) formed first. With the help of DFT calculations, we calculated the activation energies for the cyclization reactions (Scheme 2).

Scheme 2. Computed Reaction Pathway

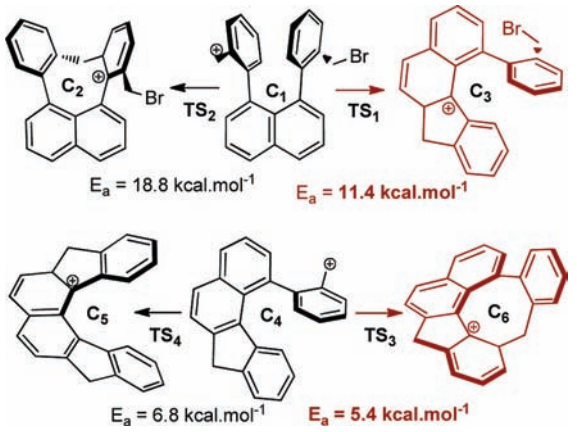

From 1,8-bisarylnaphthalene, the five-membered ring is favored over the eight-membered product and the activation energies are found to be respectively ($\mathbf{TS_1}$) 11.4 and ($\mathbf{TS_2}$) 18.8 kcal·mol^{-1}. A possible explanation of this result is a better stabilization of the charge on the naphthalene unit in the five-membered transition state than on the phenyl group in the eight-membered transition state.

In a second step and starting from the five-membered intermediate $\mathbf{C_4}$, the energy barriers for cyclization leading to the five/eight product is found to be ($\mathbf{TS_3}$) 5.4 kcal·mol^{-1}, a value significantly lower than the energy barrier calculated for the formation of the five/five product (($\mathbf{TS_4}$) 6.8 kcal·mol^{-1}). The HOMO of the five-membered compound $\mathbf{C_4}$ is mainly localized on the D and C rings of the benzo[*c*]fluorenyl unit while no contribution is observed on the A ring (Figure 3).

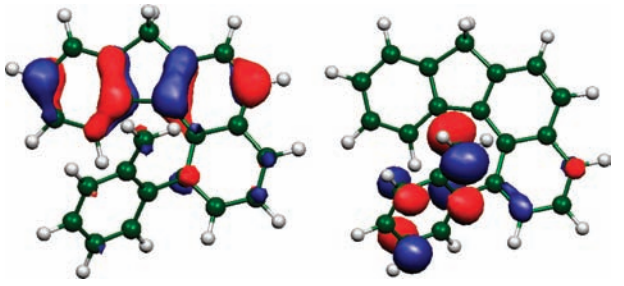

Figure 3. Frontier orbital contour plots of the five-membered cation $\mathbf{C_4}$. The contour threshold is set to 0.05 au, and these orbitals have been computed at the B3LYP/6-31G(d) level.

Therefore a better HOMO−LUMO interaction is expected in the five/eight transition state and may explain the calculated selectivity. Due to the curved shape of the benzo[*c*]fluorenyl core as evidenced by X-ray analysis, **5** and **6** can be considered as helical architectures displaying potential racemization energy barriers (REBs).

In the more classical carbohelicene series, the REB mainly depends on two factors: the number of ortho-fused rings[8] and modulation of steric hindrance on terminal positions of the inner helix.[9,10] As molecules **5** and **6** display both factors, it was thus of high interest to determine their REB and rank such architecture into a classical carbohelicene REB scale. With this aim, the geometry of the racemization transition state (RTS) has been optimized at the B3LYP/6-31G(d) level. The RTS is strongly twisted explaining the unexpected high calculated REB value of 31 kcal·mol^{-1} (see SI).

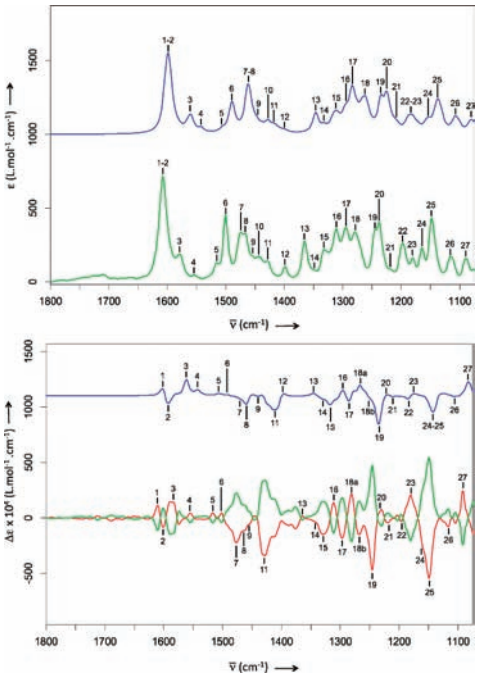

Figure 4. IR and VCD spectra of **6** calculated for the (*M*) enantiomer (in blue) and measured in $CDCl_3$ for the first eluted (in green) and the second eluted (in red) enantiomers.

The enantiomers of compound **6** were separated by analytical liquid chromatography on a chiral stationary phase. Semipreparative resolution was then performed to obtain a few milligrams of each enantiomer with an ee higher than 97%. The first eluted enantiomer corresponds to the (+)$ECD_{254\ nm}$ form according to the CD detection in the mobile phase. Modest specific rotations were measured for the first and second eluted enantiomers (in $CHCl_3$ at different wavelengths, see SI). The enantiomerization barrier of compound **6** was determined in refluxing butan-1-ol, $\Delta G^{\ddagger} = 31.4$ kcal·mol^{-1} (117 °C, butan-1-ol), in excellent agreement with the calculated barrier. IR and VCD

(8) Martin, R. H.; Marchant, M. J. *Tetrahedron* **1974**, *30*, 347.
(9) Janke, R. H.; Haufe, J. H.; Würthwein, E.-U.; Borkent, J. H. *J. Am. Chem. Soc.* **1996**, *118*, 6031.
(10) Pieters, G.; Gaucher, A.; Marque, S.; Maurel, F.; Lesot, P.; Prim, D. *J. Org. Chem.* **2010**, *75*, 2096.

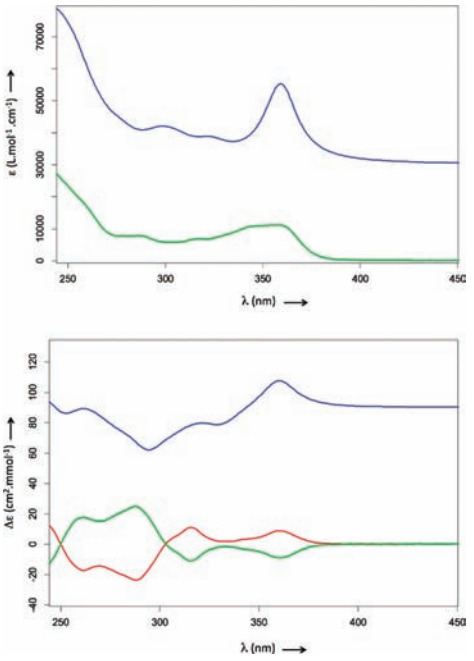

Figure 5. UV and ECD spectra of **6** calculated for the (*M*) enantiomer (in blue) and measured in $CHCl_3$ for the first eluted (in green) and the second eluted (in red) enantiomers.

spectra of the enantiomers were measured and compared with the calculated spectra for (*M*)-**6**. The geometry optimizations, vibrational frequencies, IR absorption, and VCD intensities were calculated with Density Functional Theory (DFT) using B3LYP combined with the TZVP basis set. A very good agreement is observed between the experimental and calculated spectra (Figure 4). The VCD spectrum of the second eluted enantiomer (red line in Figure 4) matches the calculated one for (*M*)-**6** (blue line in Figure 4).

UV and ECD spectra of the enantiomers were recorded in chloroform and calculated for (*M*)-**6** using TDDFT with the CAM-B3LYP functional and 6-31++G(d,p) basis set. Comparison between experimental and calculated spectra, particularly, the bands at 290 and 360 nm, confirm the assignment of the (*M*) configuration to the second eluted enantiomer (Figure 5).

In conclusion, we described the synthesis and properties of new nonsymmetrical polycyclic architectures that display both helicity and a saddle-type shape. The unprecedented molecular chiral architecture is based on a cylooctatriene core surrounded by an association of benzo[*c*]fluorene and *ortho*-phenylene units. The reaction pathway has been determined and evidenced the formation of the five-membered ring prior to the construction of the cyclooctatriene fragment. The enantiomers were stable enough to be isolated by chiral chromatography and were fully characterized. The absolute configuration, chiroptical properties, and enantiomerization barrier of these new chiral polycyles have been closely examined.

Acknowledgment. Authors gratefully thank MENRT, CNRS, and the University of Versailles-St-Quentin-en-Yvelines for a grant (G.P.) and financial support.

Supporting Information Available. Experimental procedures, characterization data including emission spectra of **5** and **6**, chiral HPLC separation, ECD, VCD, and enantiomerization barrier for the enantiomers of **6**, full geometry and energy information in the form of GAUSSIAN 03 archive entries. This material is available free of charge via the Internet at http://pubs.acs.org.